NASA

Technical Memorandum 82123

Infrared Radiative Transfer through a Regular Array of Cuboidal Clouds

Harshvardhan
James A. Weinman

MAY 1981

National Aeronautics and
Space Administration

Goddard Space Flight Center
Greenbelt, Maryland 20771

INFRARED RADIATIVE TRANSFER THROUGH A REGULAR ARRAY OF CUBOIDAL CLOUDS

Harshvardhan[1,2] and James A. Weinman[3]

[1]Department of Meteorology, University of Maryland, College Park, MD 20742
[2]Laboratory for Atmospheric Sciences, Goddard Space Flight Center, Greenbelt, MD 20771
[3]Space Science and Engineering Center, University of Wisconsin, Madison, WI 53706

May 1981

GODDARD SPACE FLIGHT CENTER
Greenbelt, Maryland 20771

CONTENTS

"Page missing from available version"

INFRARED RADIATIVE TRANSFER THROUGH A REGULAR ARRAY OF CUBOIDAL CLOUDS

Harshvardhan and James A. Weinman

ABSTRACT

A study has been made of infrared radiative transfer through a regular array of cuboidal clouds which considers the interaction of the sides of the clouds with each other and the ground. The theory is developed for black clouds and is extended to scattering clouds using a variable azimuth two-stream (VATS) approximation (Harshvardhan et al., 1981). It is shown that geometrical considerations often dominate over the microphysical aspects of radiative transfer through the clouds. For example, the difference in simulated 10μm brightness temperature between black isothermal cubic clouds and cubic clouds of optical depth 10, is less than 2° for zenith angles less than 50° for all cloud fractions when viewed parallel to the array.

The results show that serious errors are made in flux and cooling rate computations if broken clouds are modeled as planiform. Radiances computed by the usual practice of area-weighting cloudy and clear sky radiances are in error by 2°-8°K in brightness temperature for cubic clouds over a wide range of cloud fractions and zenith angles. It is also shown that the lapse rate does not markedly affect the exiting radiances for cuboidal clouds of unit aspect ratio and optical depth 10.

INFRARED RADIATIVE TRANSFER THROUGH A REGULAR ARRAY OF CUBOIDAL CLOUDS

1. Introduction

Radiative parameterization of clouds is required for climate and general circulation models because clouds represent the most variable quantity that affects radiative fluxes. To date, all general circulation models have utilized plane parallel theory to construct cloud parameterizations even though it has been realized that a significant portion of the total cloud field is broken and individual cloud elements have horizontal dimensions of the same order as their height. In these cases, the assumption of infinite horizontal extent in solving the radiative transfer equation is invalid and parameterizations based on plane parallel theory must be regarded as suspect.

The particular case of monochromatic radiative transfer through single cuboidal clouds has been studied in both solar and infrared wavelengths (McKee and Cox, 1974; Davies, 1978; Liou and Ou, 1979 and Harshvardhan et al., 1981). However, each element in a broken cloud field cannot be considered independently as there is cloud-cloud interaction. The problem of infrared transfer through an array of black clouds has been dealt with extensively in the Estonian literature (Ohvril and Epik, 1978). Ellingson and Kolczynski (1980) have computed infrared heating rates in the atmosphere in the presence of an array of black cylindrical clouds. Interpretation of infrared radiances measured by satellite borne sensors also requires an understanding of the effects of the finite horizontal extent of clouds.

The present study considers a regular array of identical cuboidal clouds, as in Aida (1977), overlying a non-reflecting surface embedded in a non-participating atmosphere. Only infrared radiative transfer is considered. The theory of transmission through the array and emission from the cloud field is first developed for black isothermal clouds. The work is then extended to 10 μm radiation interacting with a field of clouds which scatter and absorb radiation. The VATS solution to the

single cloud problem employed by Harshvardhan et al. (1981) is used. Computations to derive both fluxes and radiances are developed as a function of the cloud fraction.

2. Radiative Transfer through an Array of Black Clouds

Consider an idealized broken cloud field in the form of an extended regular array of cuboids. A portion of this array is illustrated in Fig. 1. Note that all elements of the array are identical and lie in one plane. Also, the horizontal dimensions of all clouds are assumed equal, although this constraint may, in principle, be relaxed. In general, the height of each element, z^*, is different from the horizontal dimension, s. From the figure, the area of the top and bottom face is $A_o = s^2$ and of each side face, $A_1 = sz^*$. We define the aspect ratio of each element as

$$a = \frac{z^*}{s} = \frac{A_1}{A_o} \tag{1}$$

If the spacing between each element is equal in the x- and y-directions as shown in the figure, then the fraction of the field covered by clouds when viewed normally, henceforth referred to as the cloud fraction is

$$N = \left(\frac{s}{s+d}\right)^2 \tag{2}$$

Consider a radiatively black cuboid at uniform temperature, T_o. The monochromatic power ($W\mu m^{-1}$) emitted to space by the top face is $\pi B_o A_o$ where B_o is the Planck emission at T_o. The monochromatic power emitted by each side face is $\pi B_o A_1$ and for a single cloud, half escapes to space and half goes to the ground. It is assumed that the atmosphere does not interact with the radiation field. This would be reasonably true in the atmospheric window centered around 10 μm. The total power emitted to space by a single cuboid is

$$P = \pi B_o A_o (1 + 2a) \tag{3}$$

where a is the previously defined aspect ratio. We define the quantity in parenthesis as the power ratio, p. However, if the cloud is part of the array shown in Fig. 1, some of the energy emitted by the side faces will be intercepted by neighboring clouds. If the fraction of energy diffusely emitted

by one side face that is intercepted by all these clouds is $\mathfrak{I}$, then the power emitted to space by each side face is $\pi B_o A_1 (1 - \mathfrak{I})/2$ and the total power emitted to space by each cuboid is

$$P = \pi B_o A_o [1 + 2a(1 - \mathfrak{I})] \tag{4}$$

so that the power ratio is

$$p = 1 + 2a(1 - \mathfrak{I}) \tag{5}$$

We now introduce the concept of effective emittance for the cuboidal array on the same lines as the emittance in plane parallel theory. Here we use power rather than flux because the emitting areas have different dimensions. We define the effective emittance of a broken cloud array as the ratio of the power emitted by a region containing the array in the absence of ground emission to the power that would be emitted if the entire area was covered by a black surface at the same temperature. If there are n identical clouds of tops A_o as in the present model, then the effective emittance is

$$\therefore \quad \mathcal{E} = \frac{nP}{\pi B_o A_t} \tag{6}$$

where A_t is the total area; but the cloud fraction is $N = nA_o/A_t$ and therefore from (4), (5) and (6), we have

$$\mathcal{E} = Np \tag{7}$$

Consider some limiting cases of the above equation. When $a \to 0$, $p \to 1$ and $\mathcal{E} = N$ and the problem reduces to the planiform case. When $N \to 1$ the clouds in the array approach each other and all the energy emitted by the side faces is intercepted, so $\mathfrak{I} \to 1$ and $p \to 1$; here, $\mathcal{E} = N = 1$. It can be seen that $\mathcal{E}$ plays the role of an effective cloud fraction, N_e, and the two can be used interchangeably for black isothermal clouds.

The effective transmittance through the array of black cuboidal clouds is

$$\mathfrak{T} = 1 - \mathcal{E} = 1 - N_e \tag{8}$$

Thus, the power emitted to space from a broken cloud array at T_o over a black ground at temperature T_1 is

$$P_{out} = \pi B_o A_t \bar{\mathcal{E}} + \pi B_1 A_t \bar{\mathcal{F}} \tag{9}$$

where B_1 is the Planck emission corresponding to T_1. Further, the flux per unit area of the field is given by

$$F_{out} = \frac{P_{out}}{A_t} = \pi B_o N_e + \pi B_1 (1 - N_e) \tag{10}$$

and the cuboidal black isothermal cloud problem takes the form of the planiform cloud model for which

$$F_{out} = \pi B_o N + \pi B_1 (1 - N) \tag{11}$$

a. Effective Cloud Fraction

If the sides of the clouds are black emitters and the clouds are isothermal, the faces will radiate diffusely and uniformly. The fraction of energy emitted by each side face that is intercepted by all the neighboring faces can be computed using the angle factors described by Sparrow and Cess (1978). A top view of the regular array is shown in Fig. 2. Due to symmetry we need only consider one side face, such as the hatched face on cloud 00 marked in the figure. A fraction of the energy emitted by this face is intercepted by the opposite face (hatched on cloud 01). All of the other hatched faces (as well as their mirror images) also intercept some fraction of this emitted energy. These fractions can be computed using angle factor tables and related equations given in the Appendix of Sparrow and Cess (1978), as long as the faces are not partially obscured. Even when there is some obscuration, the faces can be divided into smaller strips so that only the irradiated areas contribute to the total configuration factor. This is best accomplished graphically for the different cloud spacings corresponding to different cloud fractions. This method of obtaining $\bar{\mathcal{F}}$ and hence, N_e, is prone to considerable error as N increases so an alternative technique was used.

The effective cloud fraction, N_e, was deduced experimentally from the transmission of a diffuse light source through an opaque array. This is the optical analog obtained by setting $B_o = 0$ in (10). For this, an array of black blocks was placed on a light table covered with a diffusing sheet. The flux

passing through the array was measured with a Tektronix Model J16 digital photometer with a cosine corrected remote illuminance probe. The probe was translated above the blocks and the mean of a number of readings was used to compute the transmission, $(1 - N_e)$, from (10). As a check on the accuracy of the experiment, the measured results for an array of infinitely long bar clouds was compared with theory which is readily available in Sparrow and Cess (1978) for this configuration. This is shown in Fig. 3 for bar clouds of unit aspect ratio. The measurements were taken by lining up a large number of black blocks in a parallel array to simulate the infinite extent in one horizontal dimension. Four sets of measurements were taken and they are shown in the figure with their respective uncertainties. Correspondence is good for $N \lesssim 0.6$, but for higher values, grazing light reflected from the side walls of the blocks which were not perfectly black. This produced higher values of the measured transmission which gave an underestimate of N_e. Figure 3 also shows the curve $N_e = N$ corresponding to planiform clouds with $a = 0$.

Measurements were then made for the regular array of cuboids shown in Fig. 2 with two different aspect ratios; the resulting N_e values are shown in Fig. 4. For comparison, the values derived from summing up the angle factors is shown for small N when there is not much obscuration and the theory is still quite accurate. If the blocks are arranged such that their corners are touching in a checkerboard pattern, then $N = 0.5$ and N_e can be obtained exactly from the expression for angle factors because each side face sees only three other faces. The comparison for this case is also shown on Fig. 4. Finally, a series of curves are empirically fitted through the available data points to represent N_e. The empirical expression

$$N_e = \frac{[1 + 2a(1 + 0.15\,N)]\,N}{1 + 2aN(1 + 0.15\,N)} \tag{12}$$

is shown in Fig. 4. The curves follow the general pattern of the results presented in Ohvril and Epik (1978) and Ellingson and Kolczynski (1980). It may be noted that as $N \to 0$, $N_e \to (1 + 2a)N$, which is the correct limit for a single cuboid (see Eq. 3). Note that simulations of various geometrical cloud configurations can be constructed so that N_e can be empirically derived as a function of N.

b. Fluxes

A consequence of the finite nature of each cloud in the array is to increase the effective cloud fraction because N_e is always greater than N. This implies that energy loss to space from a broken cloud array is less than that computed using the cloud fraction without considering the sides of the clouds.

The effective black body emission temperature at 10 μm from a region containing the model cloud array at 255°K overlying a black ground at 290°K is shown in Fig. 5. The curve marked a = 0 is the planiform case. It is evident that errors in flux of 5°-10° equivalent temperature can be made for clouds of unit aspect ratio. This significantly affects the radiation balance because radiative models incorrectly weight clear and overcast fluxes as in (11). If a significant portion of the global cloud cover is broken, then $(F_{out})_{cuboidal} < (F_{out})_{planiform}$. This is especially important for simulations of the Earth Radiation Budget Experiment.

c. Net Flux Divergence

Of possible impact in dynamic models is the fact that the cooling rate across the cloud layer is different from the planiform case because of the radiation intercepted by the sides of the cloud (Ellingson and Kolczynski, 1980). If a regular array of black isothermal clouds at T_o is embedded in a non-participating atmosphere over a ground at T_1, then the difference in net flux between the top and bottom of the cloud layer is

$$\Delta F_{net} = \pi \mathcal{E} (2B_o - B_1) \tag{13}$$

where $\mathcal{E}$ is the effective emittance of the layer and B_o and B_1 are the Planck functions at T_o and T_1 respectively. It follows from (13) that the cooling rate across the layer, calculated for the cuboidal cloud model is related to that obtained using the planiform assumption by

$$\frac{(\Delta F_{net})_{cuboidal}}{(\Delta F_{net})_{planiform}} = \frac{N_e}{N} \tag{14}$$

This quantity is plotted in Fig. 6 for various aspect ratios as a function of the cloud fraction, N. It is evident that for cumulus cloud fields with N = 0.3, which is a typical value, the cooling rate in the atmospheric window could be two to three times that derived from the planiform cloud assumption.

d. Radiances

If the array is composed of black isothermal cubic clouds, the radiance in any direction depends on the field of view obscured by the clouds. When viewed from above, only the cloud fraction N obscures the ground, whereas from any lower observation angle, the sides of the cloud also obscure the ground. This effect is shown in Fig. 7 for two viewing directions; $\phi = 0°$, in which the observer views parallel to the array seeing only the top and one side face of each cloud, and $\phi = 45°$, which is a diagonal view in which the top and two adjacent side faces are seen. Individual curves are marked with the cloud fraction; the aspect ratio is unity. The cuboids are at 255°K while the ground is at 290°K.

The radiance profile is governed exclusively by geometry; the sharp kink in the individual curves is at the angle beyond which the underlying ground is completely obscured in the viewing direction. At higher zenith angles, for $\phi = 0°$, the radiance is

$$I = \sqrt{N}\, B_0 + (1 - \sqrt{N})\, B_1 \qquad (15)$$

Only two cases are shown for $\phi = 45°$ because the geometrical arrangement is very complex, but that is sufficient to illustrate the effect of viewing direction. The radiance drops off much more rapidly for this case. Figure 7 suggests that the brightness temperature measured by a satellite instrument cannot be related to the cloud top temperature for broken cloud fields without considering the geometry of the array and the viewing direction if the field of view includes a number of cloud elements.

3. Monochromatic Radiative Transfer through an Array of Non-Black Clouds

a. Isothermal Clouds

Let us now consider a regular array as in Fig. 1 but we introduce the requirement that the cloud is a cuboid of water droplets with a size distribution characterized as C-1 by Deirmendjian (1969).

The radiative properties at 10 μm of such cloud droplets are computed from Mie theory. Unlike the black blocks of Section 2, these clouds are partially transparent to 10 μm radiation. It is also assumed that the clouds in the array are identical and isothermal while the ground below is non-reflecting. It will be shown that the results of the previous section can be used to obtain fluxes and radiances emanating from such an array.

The thermal radiation emerging from cuboidal clouds was determined by means of the VATS technique of Harshvardhan et al. (1981). It is sufficient to note here that fluxes leaving the faces of the cuboid may be expressed in terms of the mean radiance, $I_o = 1/4\pi \int_0^{4\pi} I d\Omega$, where Ω is the solid angle. I_o is obtained from the solution of

$$\nabla^2 I_o = \lambda^2 (I_o - B_o) \tag{16}$$

where

$$\lambda = k[3(1 - \tilde{\omega})(1 - \tilde{\omega} g)]^{1/2}$$

with k, $\tilde{\omega}$ and g being the extinction coefficient, single scattering albedo and asymmetry parameter, respectively.

b. Boundary Conditions

The boundary conditions for the problem are defined by the fluxes incident on each face. In general, the flux in any direction is a function of position, say F(x, y, z) and in particular, the flux exiting each side face is a function of position on the face. For a cloud of equal sides, s, and height z*, with the origin at the center of the base, we have $(F_{x+,x+})_{x=s/2} = F(y, z)$. The flux nomenclature used here is that of Davies (1978) and Harshvardhan et al. (1981). The first subscript identifies the face while the second subscript identifies the direction.

The flux boundary conditions at the top and bottom faces are as for the single cloud, i.e.

$$(F_{z+,z-})_{z=z^*} = 0 \tag{17}$$

and

$$(F_{z-,z+})_{z=0} = \pi B_1 \tag{18}$$

with B_1 the ground emission. The average flux exiting the side face at $x = s/2$ is

$$(\bar{F}_{x+,\,x+})_{x=s/2} = \frac{1}{sz^*} \int_0^{z^*} \int_{-s/2}^{s/2} F_{x+,x+}(y, z)\, dy\, dz \tag{19}$$

If the regular array is made up of identical cuboids, then by symmetry, $(\bar{F}_{x\pm,x\pm})_{x=\pm s/2} = (\bar{F}_{y\pm,y\pm})_{y=\pm s/2}$, and this may now be used to specify the side boundary conditions.

The side faces receive radiant flux from neighboring clouds as well as that portion of the ground that is not obstructed by those clouds. If we assume that the flux exiting the side faces is isotropic and uniform over the face, it is possible to compute the incident flux on each side face of the cloud. Let A_1 be the area of each side face and A_2 the total area of all the faces visible from this face for a particular cloud fraction. Figure 2 shows that A_2 varies with the configuration because of partial obscuration by nearby clouds. The energy per unit area falling on A_1 that is diffusely emitted by A_2 is $(\bar{F}_{x+,x+})_{x=s/2}\, \mathfrak{F}_{21}\, A_2/A_1$, where $\mathfrak{F}_{21}$ is the angle factor between A_2 and A_1 defined as the fraction of energy diffusely emitted by A_2 falling on A_1. By reciprocity (Sparrow and Cess, 1978)

$$\frac{\mathfrak{F}_{21}\, A_2}{A_1} = \mathfrak{F}_{12} \tag{20}$$

and $\mathfrak{F}_{12}$ is identical with $\mathfrak{F}$ of Eq. (4) et seq. Therefore, to the extent that the cloud faces may be approximated by isotropic emitters of uniform flux, the side boundary condition for the array problem is written as

$$(F_{x+,x-})_{x=s/2} = \mathfrak{F}(\bar{F}_{x-,x-})_{x=-s/2} + (1 - \mathfrak{F})\, \frac{\pi B_1}{2} \tag{21}$$

In (21), $(F_{x+,x-})_{x=s/2}$ is the incoming flux at the $x = s/2$ face whereas $(\bar{F}_{x-,x-})_{x=-s/2}$ is the mean exiting flux out of the opposite face at $x = -s/2$.

It is necessary to examine the two assumptions made in deriving (21). The assumption of isotropy can be justified to a certain extent if the cloud is sufficiently thick, $kz^* \geq 10$, so that the upward and downward components of the mean side flux are nearly equal. This is because the radiant

flux is emission dominated. Moreover, the problem would become far more intractable if the angular distribution were to be accurately considered.

The assumption of uniform flux over the side face is not correct for single clouds (see Harshvardhan et al., 1981). As the cloud fraction increases and the spacing decreases, an error will be introduced by assuming that the mean flux is incident on the neighboring cloud. In the limit that the cloud sides touch each other, the input to one side face is the output of the opposite face, point for point, i.e.

$$(F_{x+,x-})_{x=s/2} = (F_{x-,x-})_{x=-s/2} \tag{22}$$

Note that if we set $\mathfrak{F} = 1$ in (21), the R.H.S. of the equation contains the mean flux and not the flux at each point.

Figure 8 illustrates the exchange geometry. We merge (21) and (22) such that it is applicable over the entire range of cloud fractions. The weighted boundary condition is

$$(F_{x+,x-})_{x=s/2} = [(1-\psi)\,(F_{x-,x-})_{x=-s/2} + \psi(\bar{F}_{x-,x-})_{x=-s/2}]\,\mathfrak{F} + (1-\mathfrak{F})\,\frac{\pi B_1}{2} \tag{23}$$

ψ is chosen to weight the incident flux; it is the ratio of two angle factors,

$$\psi = \frac{\mathfrak{F}_{A_j - dA_i}}{\mathfrak{F}_{dA_j - dA_i}} = \frac{d^2}{sz^*}\,4\pi G(a,N) \tag{24}$$

where the function

$$G(a,N) = \frac{1}{2\pi}\left\{\frac{(a/2R)}{\sqrt{1+(a/2R)^2}}\,\tan^{-1}\left[\frac{(1/2R)}{\sqrt{1+(a/2R)^2}}\right]\right.$$

$$\left. + \frac{(1/2R)}{\sqrt{1+(1/2R)^2}}\,\tan^{-1}\left[\frac{(a/2R)}{\sqrt{1+(1/2R)^2}}\right]\right\} \tag{25}$$

with $R = d/s = 1/\sqrt{N} - 1$ and $a = z^*/s$, the aspect ratio (This expression is given in the Appendix of Sparrow and Cess, 1978). An infinitesimal area dA_i receives flux F from an element dA_j exactly opposite it and flux $\bar{F}$ from the whole opposite face A_j. Figure 9 shows that ψ tends to unity as N becomes small and tends to zero as the faces approach each other. The precise weight in boundary condition (23) and choice of ψ is somewhat arbitrary but is physically reasonable. The contribution to

the flux arriving at a point on the sides of the clouds from any point on the opposite face depends on the angle factor between the points. In an approximate sense, the mean flux may thus be identified with the angle factor between the opposite face as a whole and the receiving point. The angle factor $\mathfrak{F}_{A_j - dA_i}$ depends on the location of dA_i but the center of the face has been used to position dA_i. For the special case which exhibits uniform flux emission, $F = \bar{F}$, and (23) reduces to (21).

c. Fluxes

The total flux emanating from the array and underlying ground can now be obtained using the single cloud solution obtained with the boundary condition (17), (18) and (23). If $(\bar{F}_{z+,\,z+})_{z=z^*}$ is the mean flux out of the top face of each cloud, then the power emitted is $A_o(\bar{F}_{z+,\,z+})_{z=z^*}$ and if $(\bar{F}_{x+,\,z+})_{x=s/2}$ is the upward component of the mean flux out of each side face, then the power emitted to space by all four sides is $4A_1(\bar{F}_{x+,\,z+})_{x=s/2}(1 - \mathfrak{F})$. Therefore, the upward flux averaged over this array may be written as

$$F_{out} = N(\bar{F}_{z+,\,z+})_{z=z^*} + 4a(1 - \mathfrak{F})\,N(\bar{F}_{x+,\,z+})_{x=s/2} + (1 - N_e)\,\pi B_1 \qquad (26)$$

If the clouds are considered black, $(\bar{F}_{x+,\,z+})_{x=s/2} = 1/2(\bar{F}_{x+,\,x+})_{x=s/2} = \pi B_o$ and (26) reduces to (10).

Computations have been made for $a = 1$ (cubic cloud) and the radiative model mentioned earlier for which the single scattering albedo, $\tilde{\omega} = 0.638$ and asymmetry parameter, $g = 0.865$ at 10 μm. Figure 10 shows the average upward flux from a regular array of cubes of optical thicknesses on each side varying from 0.5 to 20. Results are presented as an effective black body temperature. These results may be compared with the curve marked $a = 1$ in Fig. 5 to note the departure from the black case. It is evident that an optical depth of 10 or greater may be approximated quite well by black cuboids.

d. Radiances

Figure 11 shows the radiance at $\phi = 0°$ for various cloud fractions for a regular array of cubic clouds of optical dimensions (ks, ks, kz*) = (10, 10, 10). The ground and cloud temperatures are the same as before and the plot may be compared with Fig. 7 which is the black case. It should be

stressed here that these solutions are not exact but VATS approximations. However, Harshvardhan et al. (1981) have shown that the approximation is good, especially for large optical depths and these non-black cuboidal cloud results appear to be reliable. The black assumption is very good for zenith angles less than 60° as can be seen from Fig. 12 which shows the difference between the brightness temperature for black and non-black clouds with a = 1. The maximum error in radiance is less than 2°K when $\theta < 60°$ for all arrays of optically thick clouds. This situation is frequently encountered in remote sensing problems.

The simulated radiance from partly cloudy fields is of the form

$$I = I_p N + B_1 (1 - N) \tag{27}$$

where I_p is the planiform solution, B_1 the ground contribution or clear sky solution and N represents the cloud fraction. If N is taken to be the cloud fraction when viewed normally, (27) will be erroneous for non-planiform clouds. To illustrate this, we have computed I according to (27) and compared it with the present solution for an array of cubic clouds of optical dimensions (10, 10, 10). The value of I_p used in (27) is the corresponding planiform solution for optical depth 10. The difference is plotted in Fig. 13. The cloud is isothermal in both cases at T_o = 255°K while the ground temperature is T_1 = 290°K. It is evident that (27) is not valid for any zenith angle and cloud fraction with errors of 4°K in brightness temperature for a typical field of N = 0.3 viewed at $\theta = 30°$. For fair weather cumulus, with a ~ 1, the geometry is more significant than the detals of the radiative transfer microphysics and good results can be obtained with the black block assumption.

e. Non-Isothermal Clouds

We have only considered isothermal clouds so far; however, it can be demonstrated that isothermality is not a serious drawback for fair weather cumulus and other cloud formations that are not extensive in the vertical direction. Consider a cuboidal cloud array with a = 1 and optical dimensions (10, 10, 10). A vertical optical depth of 10 at 10 μm corresponds to a maximum vertical dimension of about 1 km (Deirmendjian, 1969), so the temperature difference between cloud top and base would be about 5°K. We therefore compute the radiance at $\phi = 0°$ from a non-black array of cuboids

($\tilde{\omega} = 0.638$, $g = 0.865$) with cloud top temperature, $T_{ot} = 255°K$, cloud base temperature, $T_{ob} = 260°K$, overlying the ground at $T_l = 290°K$ and compare this with the isothermal black cuboid radiance with $T_o = 290°K$.

The difference curves are shown in Fig. 14, which is very similar to Fig. 12, the isothermal comparison. Again, the maximum error is only a little more than 2°K for $\theta < 60°$. One reason that the lapse rate is not very important for sufficiently opaque clouds is that for small values of θ, the bulk of the radiation is emitted from the top and for larger zenith angles, only the upper portion of the sides are visible, the rest being obscured by neighboring clouds. In so far as clouds are optically thick, replacing a broken cloud array by black emitters at the same temperature as the cloud top is superior to the use of (27) in computing exiting radiances.

4. Summary

The results presented here show that it is possible to model the infrared radiation emanating from a broken cloud field if only the geometry of the array and the cloud top temperature are defined. Although a very simple regular array of cuboids was considered, this study compares a black cloud and a scattering-absorbing water cloud with appropriate radiative properties. The non-black problem was solved by extending the single cloud solution as obtained by a two-stream approximation to an array solution with mutual interaction. One conclusion of this study is that clouds may be approximated by black opaque finite emitters in the infrared if the optical dimensions exceed 10 on each side. This will be particularly useful in modeling irregular arrays of non-uniform sized clouds. It was also shown that a simple area-weighting of overcast and clear sky radiances for broken cloud field radiative simulations is highly erroneous when the aspect ratio of the cloud elements is about 1 or larger.

ACKNOWLEDGMENTS

This research was supported by funding provided by ARO-D grant DRXRO-DRP-15227-GS- and NASA contract NAS5-26463. We thank these agencies for their support.

REFERENCES

Aida, M., 1977: Reflection of solar radiation from an array of cumuli. J. Met. Soc. Japan, 55, 174-181.

Davies, R., 1978: The effect of finite geometry on the three-dimensional transfer of solar irradiance in clouds. J. Atmos. Sci., 35, 1712-1725.

Deirmendjian, D., 1969: Electromagnetic Scattering on Spherical Polydispersions. Elsevier, New York, 290 pp.

Ellingson, R. G., and E. Kolczynski, 1980: Cumulus clouds and infrared heating of the atmosphere Preprints of the International Radiation Symposium. Fort Collins, CO, 474-476.

Harshvardhan, J. A. Weinman, and R. Davies, 1981: Transport of infrared radiation in cuboidal clouds. submitted to J. Atmos. Sci.

Liou, K.-N., and S.-C. Ou, 1979: Infrared radiative transfer in finite cloud layers. J. Atmos. Sci., 36, 1985-1996.

McKee, T. B., and S. K. Cox, 1974: Scattering of visible radiation by finite clouds. J. Atmos. Sci., 31, 1885-1892.

Ohvril, H. A., and R. S. Epik, 1978: Description of the variability of the parameters of cumulus cloudiness and long-wave radiation averaged over the azimuth by the use of eigenvectors. Variability of Cloudiness and Radiation Field, IFA ANESSR, Tartu, 5-22. (in Russian).

Sparrow, E. M., and R. D. Cess, 1978: Radiation Heat Transfer. McGraw Hill, New York, 366 pp.

Weinman, J. A., and R. Davies, 1978: Thermal microwave radiance from horizontally finite clouds of hydrometeors. J. Geophys. Res., 83, 3099-3107.

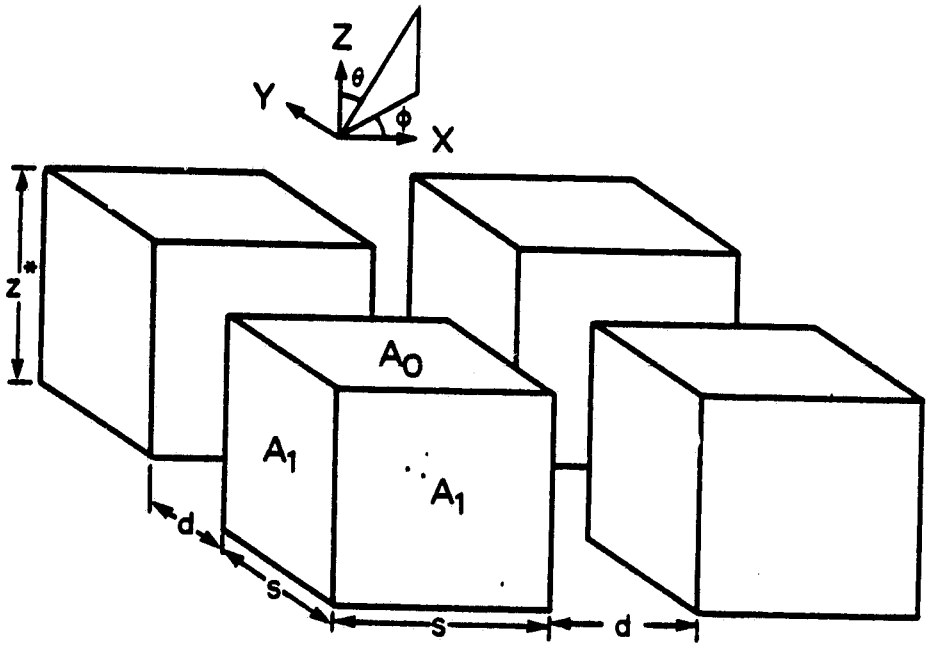

Figure 1. Schematic showing regular array of cuboids.

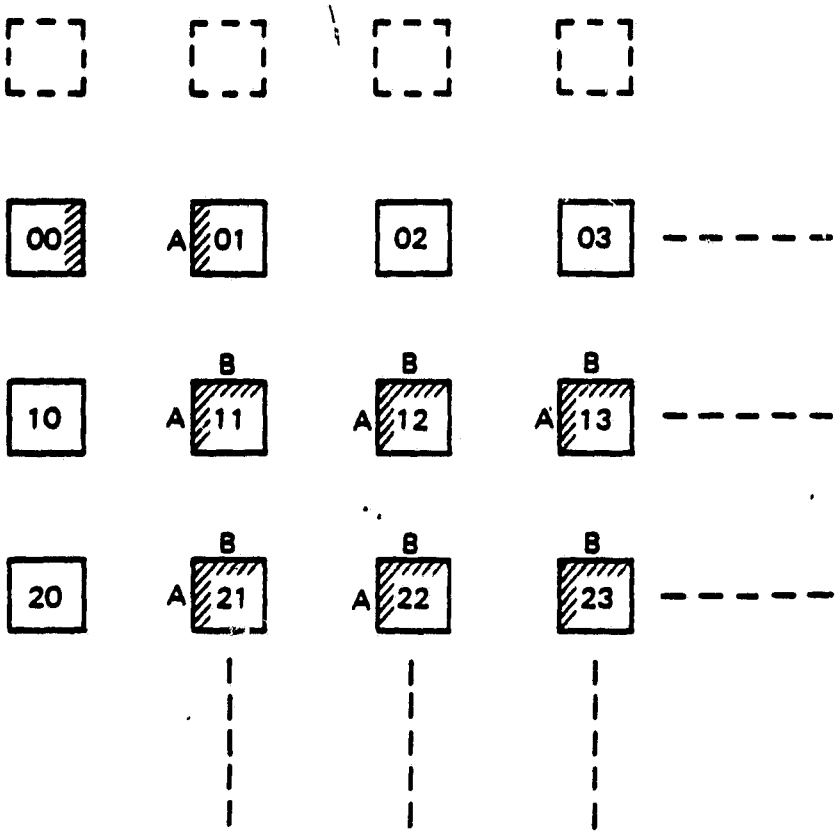

Figure 2. Top view of array showing cloud faces visible from hatched face on element 00.

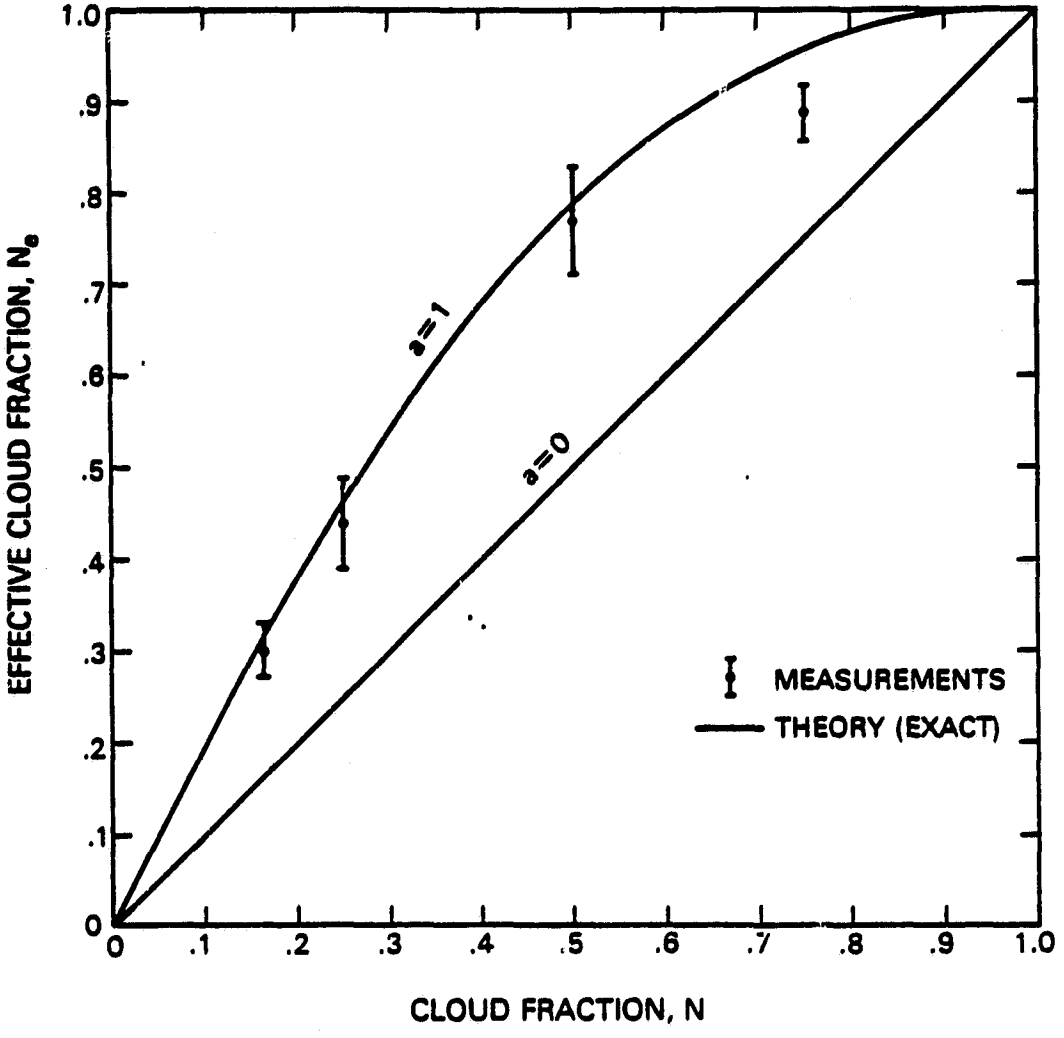

Figure 3. Effective cloud fraction for black bar clouds. Comparison of theory and measurements is for a = 1.

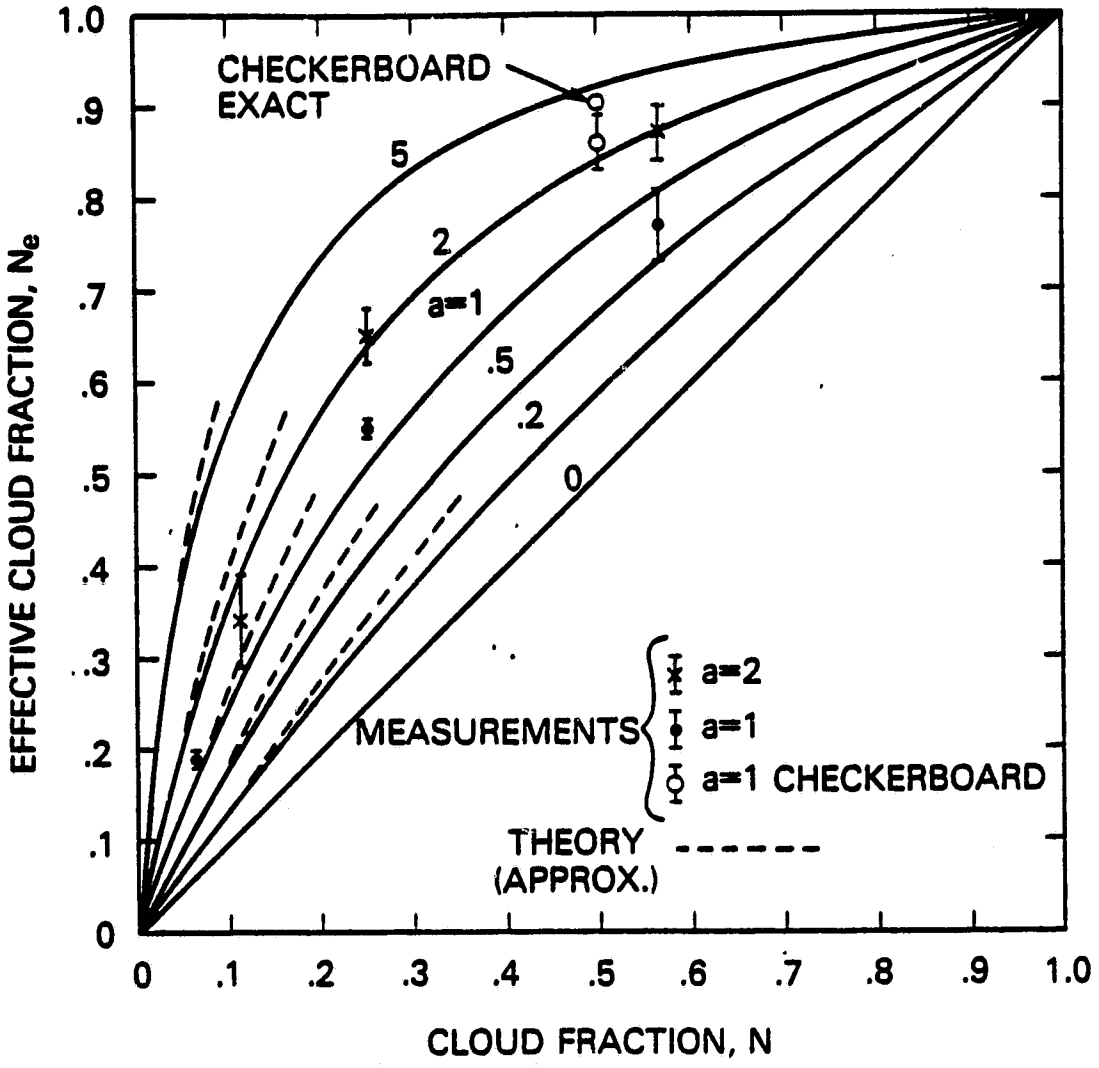

Figure 4. Effective cloud fraction for black cuboidal clouds, N_e, as a function of cloud fraction, N, for aspect ratios marked on curves. Full lines are given by Eq. 12 in text.

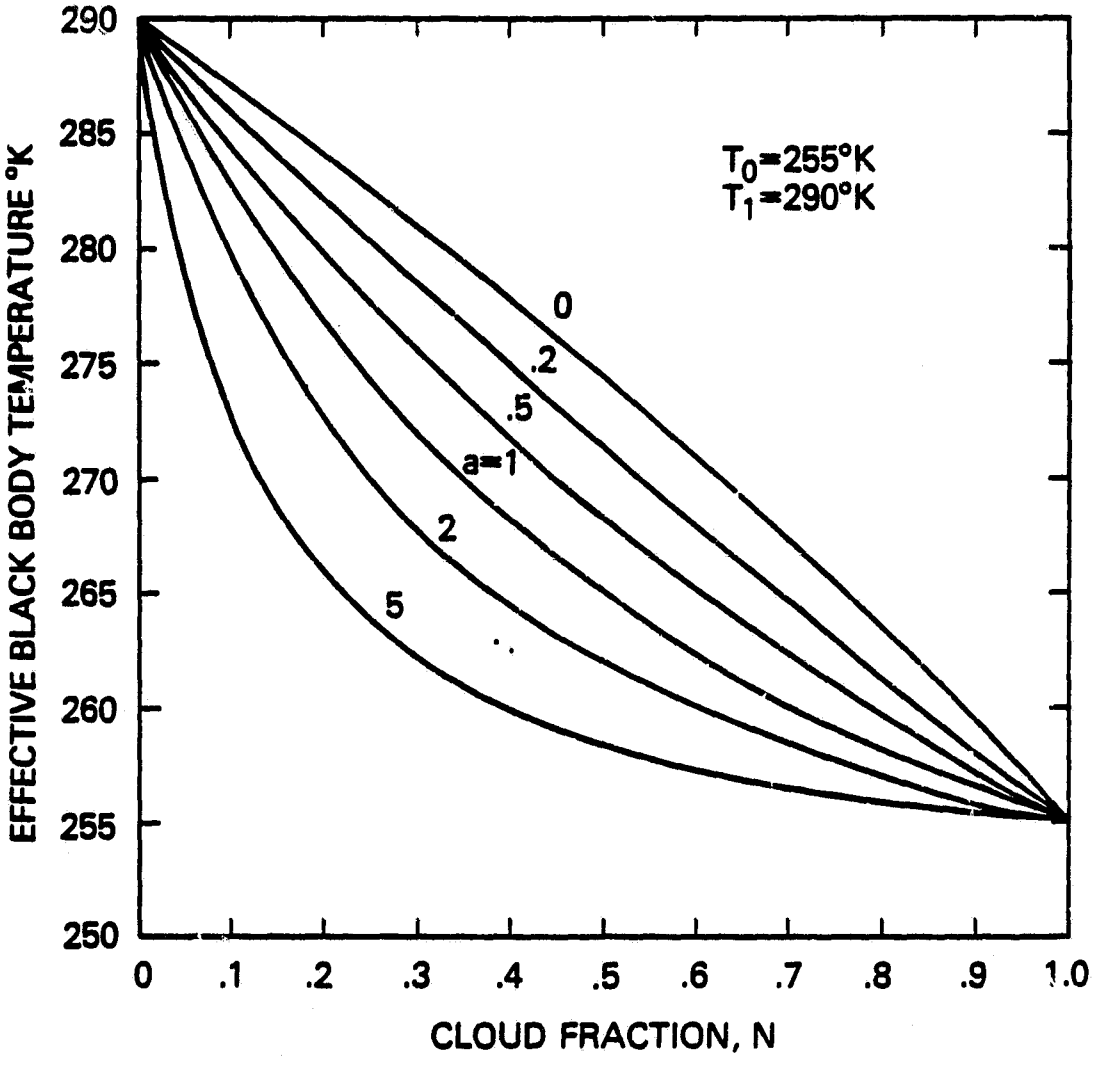

Figure 5. Upward flux from an array of black cuboids expressed as effective black body temperature for T_o = 255°K and T_1 = 290°K. Aspect ratios are marked on individual curves.

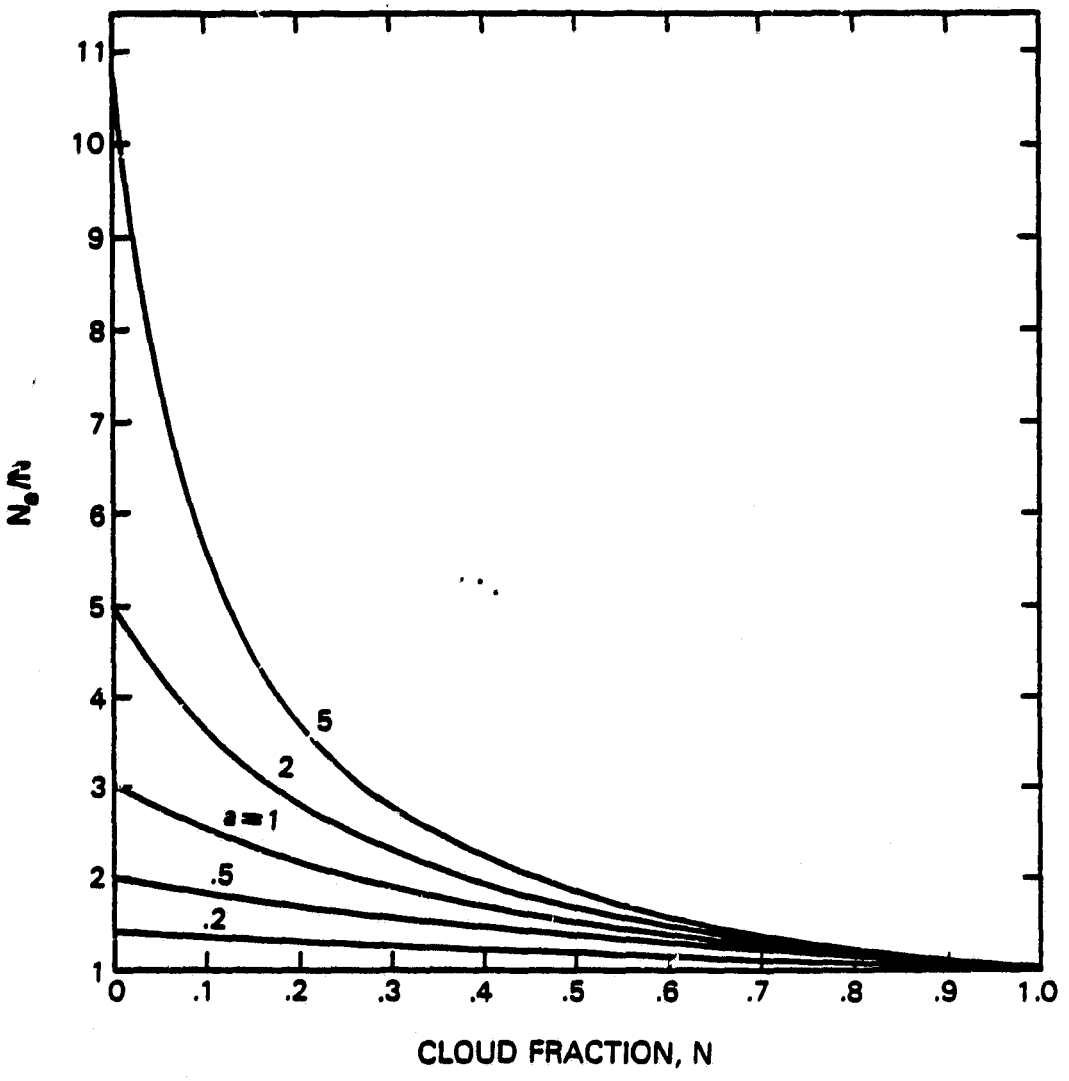

Figure 6. Ratio of cuboidal and planiform model cooling rates, N_e/N, as a function of cloud fraction, N. Aspect ratios are marked on individual curves.

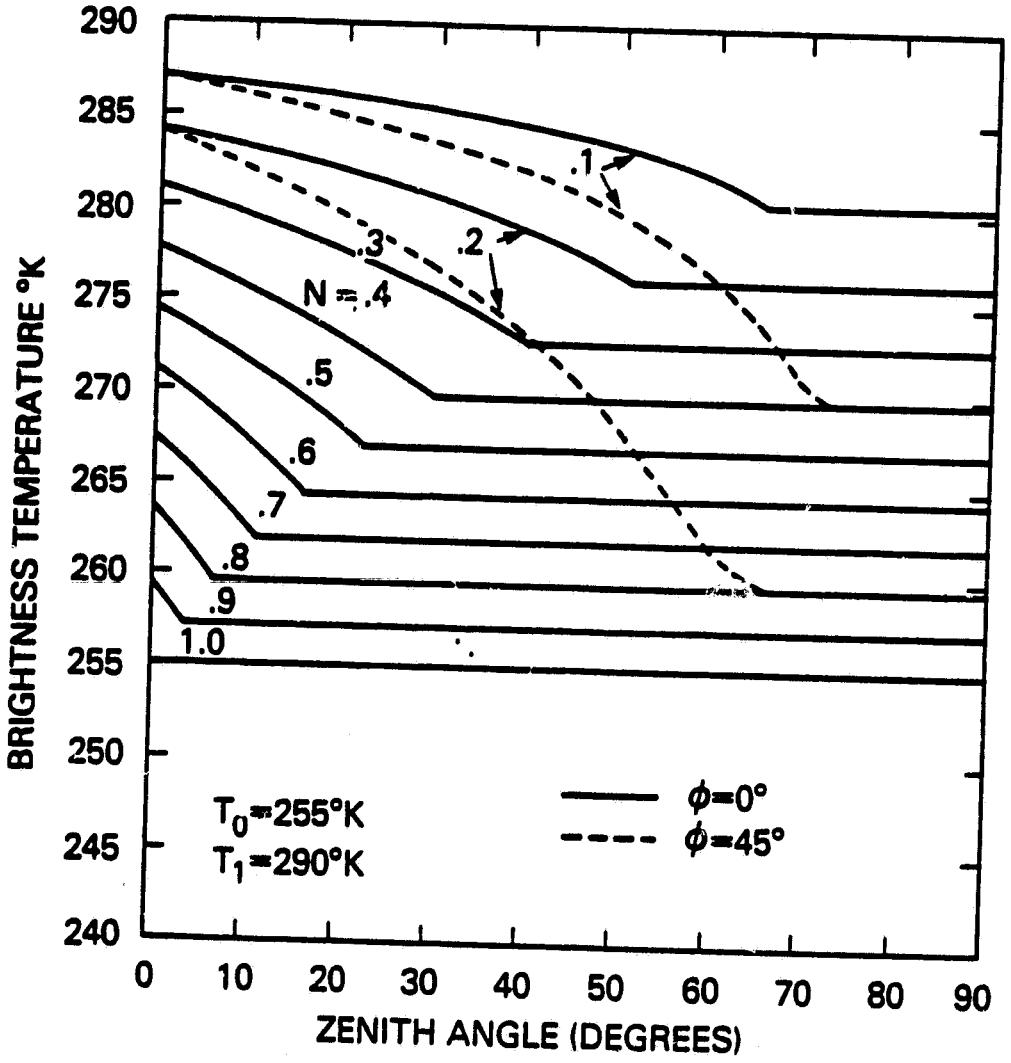

Figure 7. Brightness temperature vs. zenith angle for an array of black cuboids of aspect ratio, a = 1. Results are for two azimuth angles, $\phi = 0°$ (——) and $\phi = 45°$ (– – –); $T_o = 255°K$, $T_1 = 290°K$. Cloud fractions are marked on individual curves.

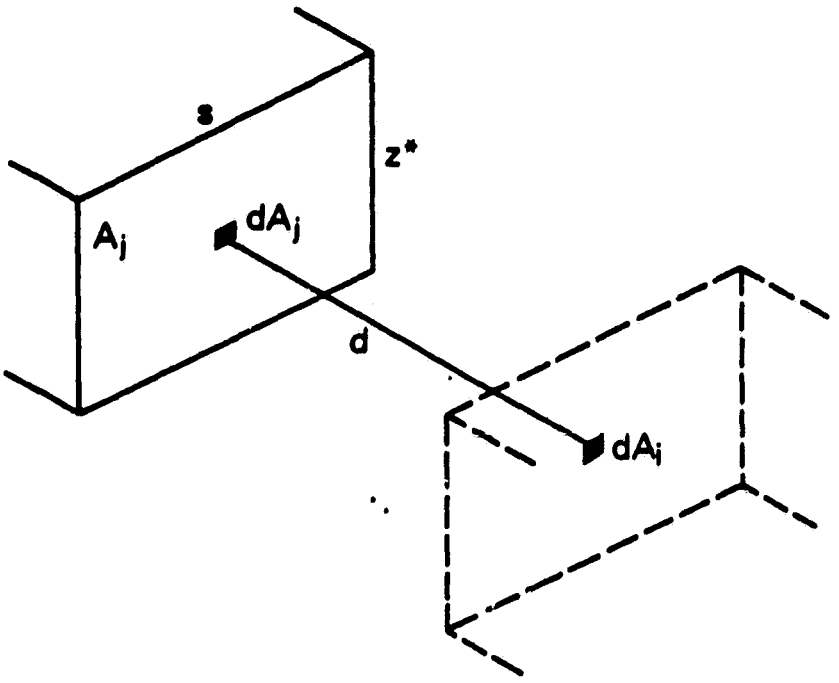

Figure 8. Geometry for energy exchange between opposite faces showing interchange between a point and the entire opposite face, and the opposite point.

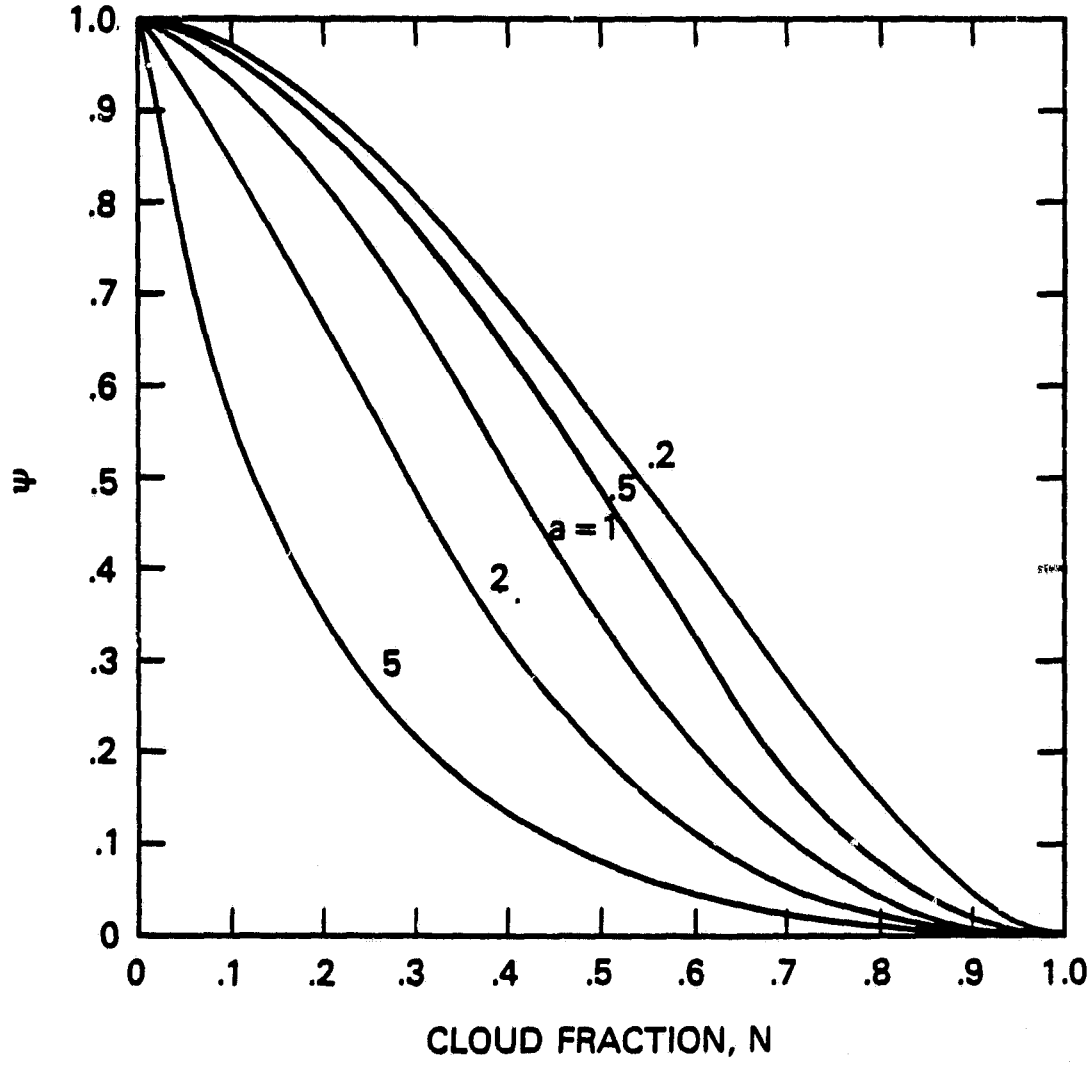

Figure 9. The function defined by Eq. 24, ψ vs N, the cloud fraction. Aspect ratios are marked on individual curves.

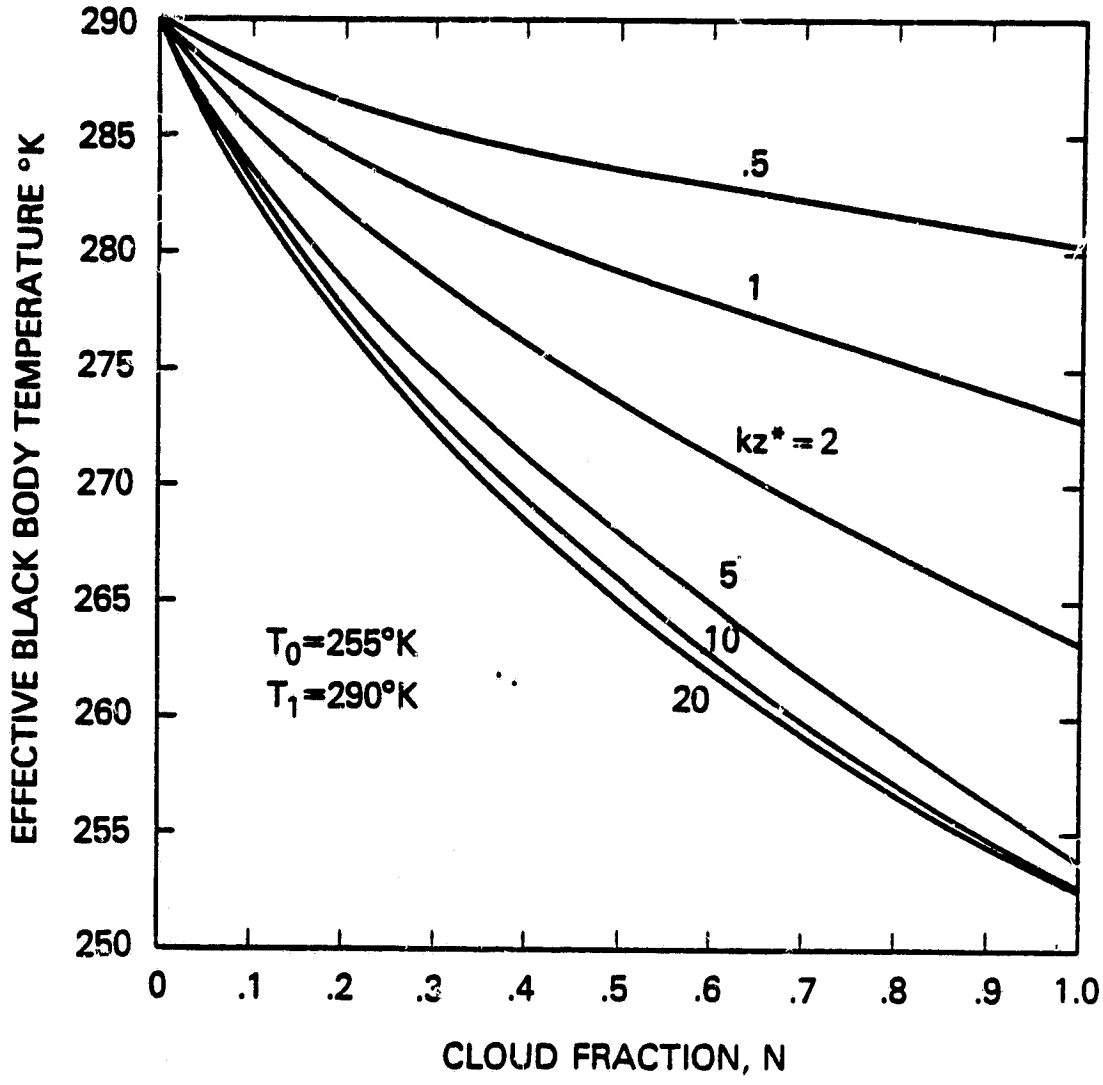

Figure 10. Same as Fig. 5 but for non-black clouds of unit aspect ratio. Radiative properties are $\tilde{\omega} = 0.638$, $g = 0.865$. Optical thickness on each side of the cuboids is marked on individual curves.

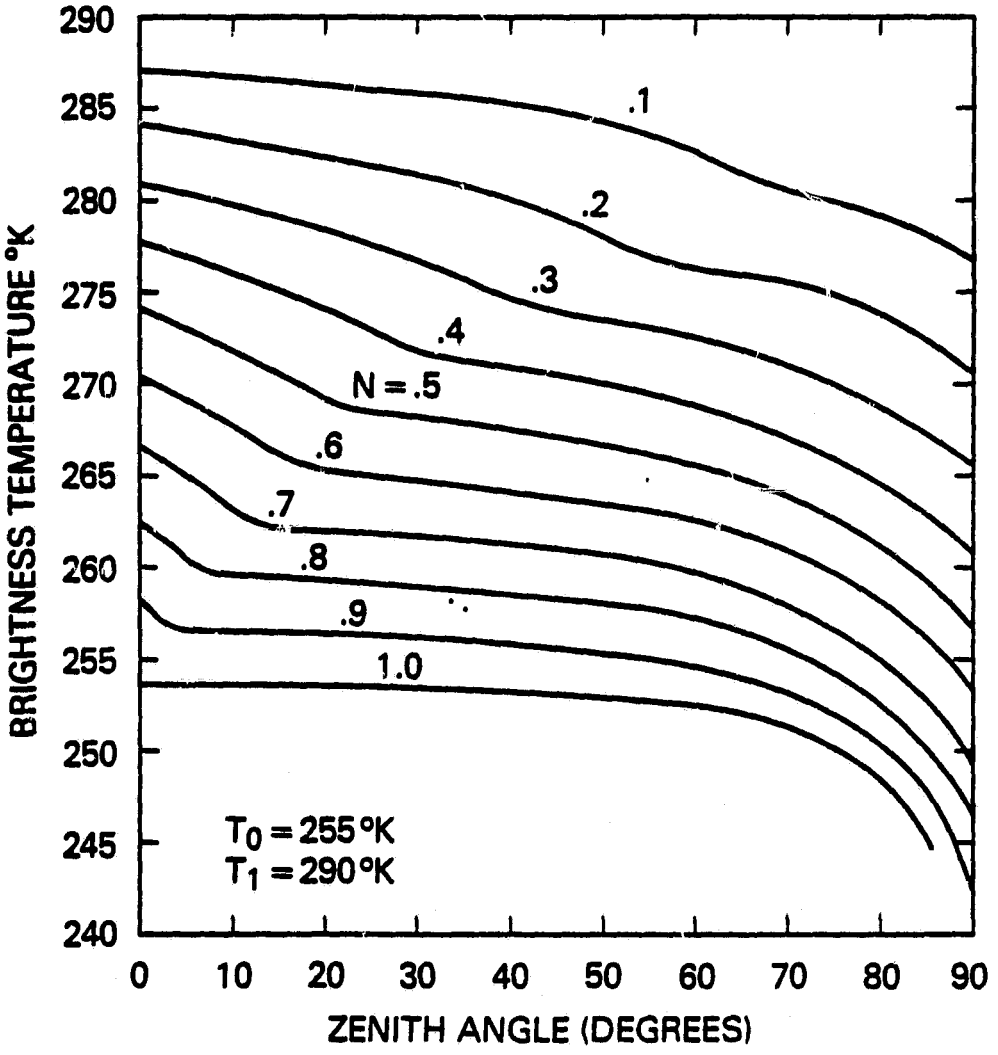

Figure 11. Same as Fig. 7 but for non-black clouds of unit aspect ratio at $\phi = 0°$. Optical dimensions are (10, 10, 10). Radiative properties are $\tilde{\omega} = 0.638$, $g = 0.865$, $T_o = 255°K$, $T_1 = 290°K$.

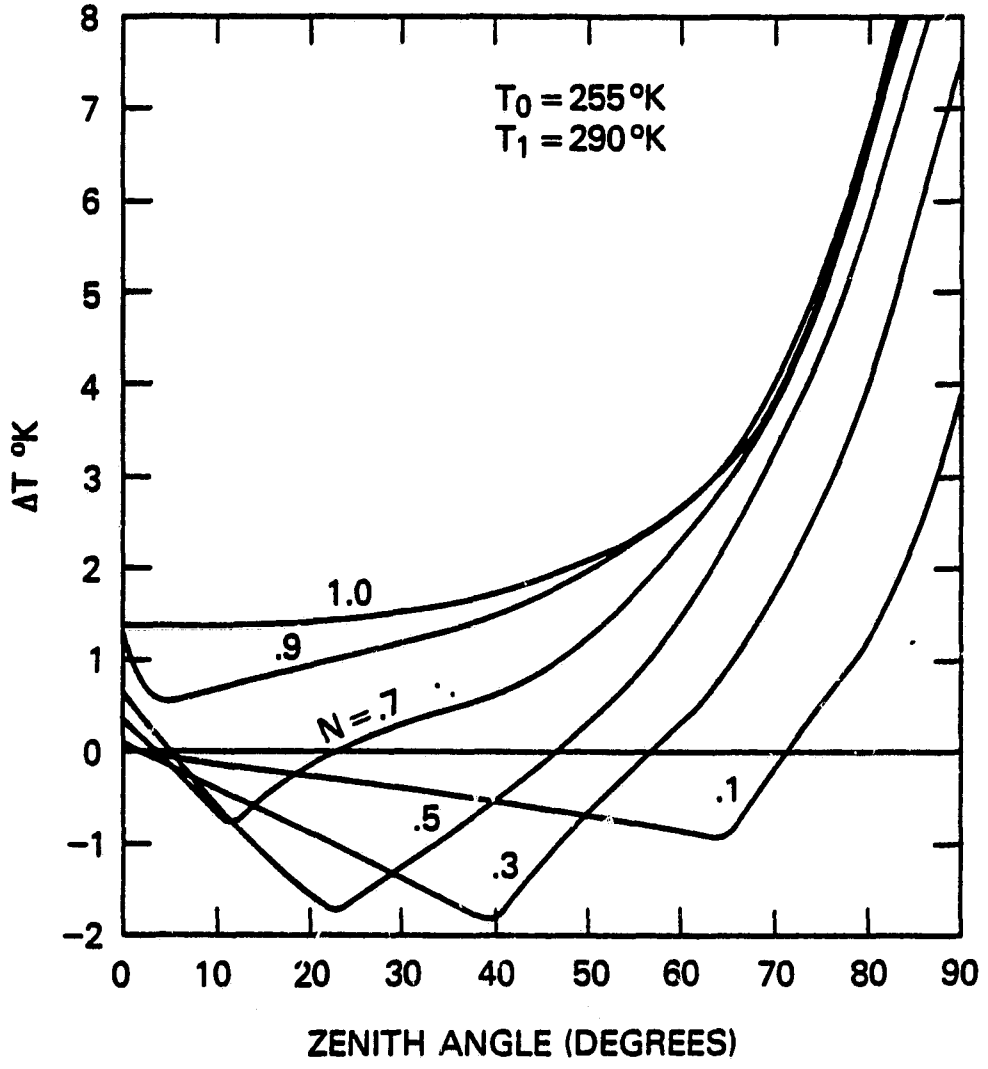

Figure 12. Difference in brightness temperature at $\phi = 0°$ between an array of isothermal black cuboids of unit aspect ratio and non-black cuboids of optical dimensions (10, 10, 10). Radiative properties of non-black cloud are $\tilde{\omega} = 0.638$, $g = 0.865$. Cloud fractions are marked on individual curves. $T_o = 255°K$, $T_1 = 290°K$.

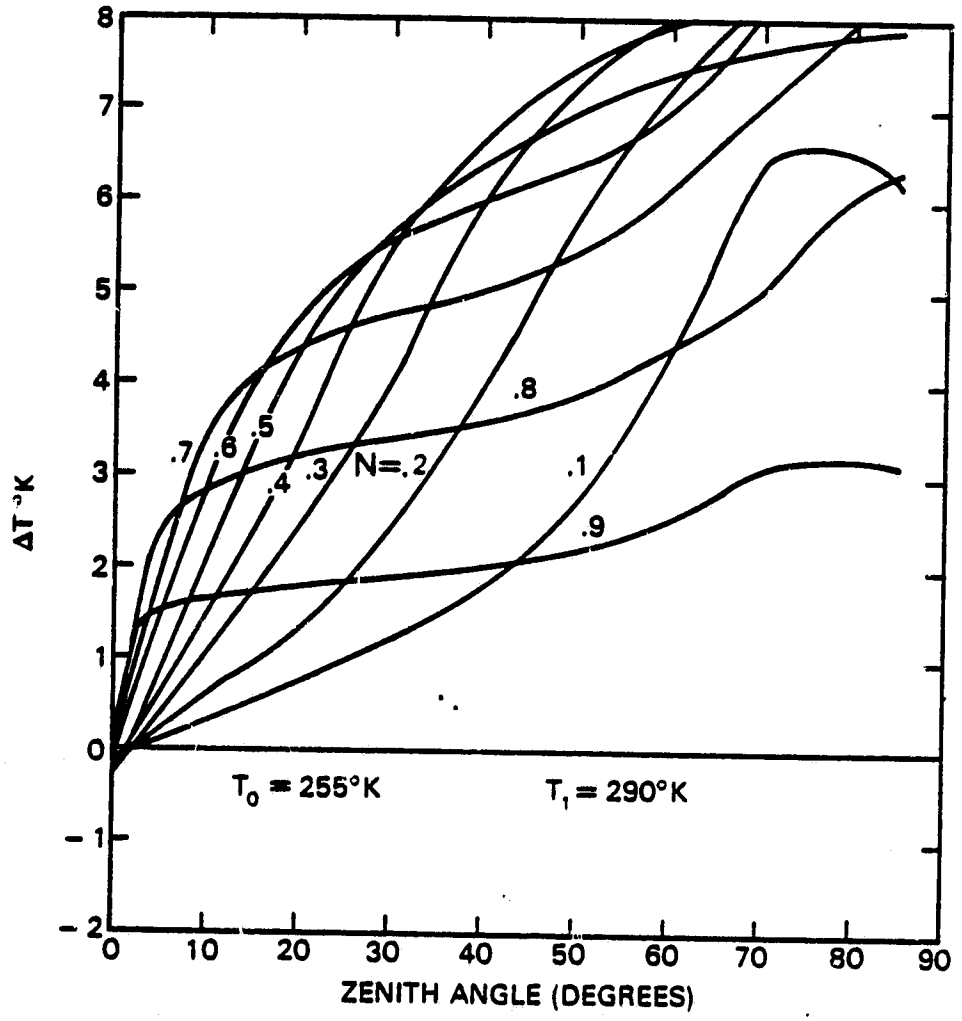

Figure 13. Difference in brightness temperature between a planiform cloud of optical thickness, kz*, equal to 10 and an array of isothermal non-black cuboids of optical dimensions (10, 10, 10) at $\phi = 0°$. Radiative properties for both clouds are $\tilde{\omega} = 0.638$, $g = 0.865$. Cloud fractions are marked on individual curves. $T_0 = 255°K$, $T_1 = 290°K$.

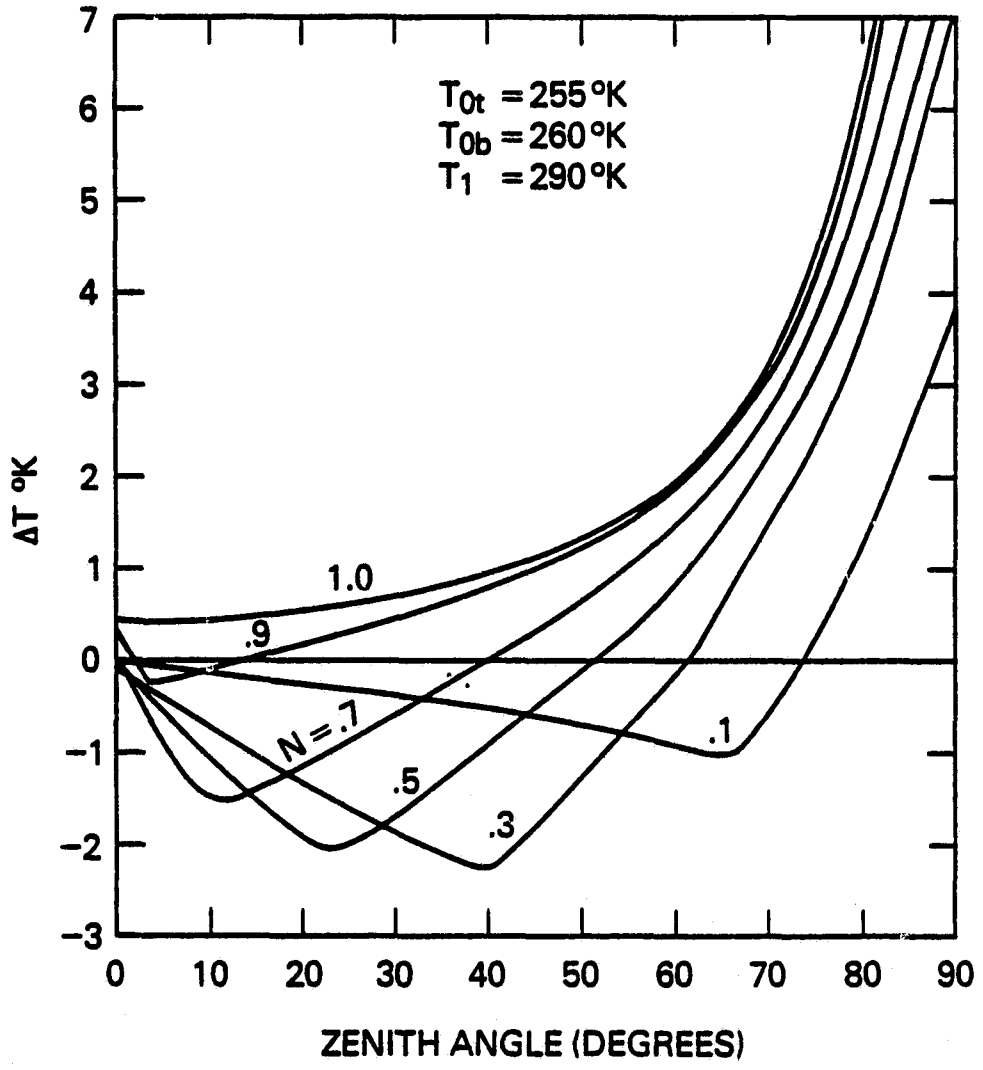

Figure 14. Same as Fig. 12 but with cloud top, T_{ot} = 255°K; cloud base, T_{ob} = 260°K; ground, T_1 = 290°K.

BIBLIOGRAPHIC DATA SHEET

1. Report No.	2. Government Accession No.	3. Recipient's Catalog No.
TM 82123		

4. Title and Subtitle	5. Report Date
Infrared Radiative Transfer through a Regular Array of Cuboidal Clouds	May 1981
	6. Performing Organization Code
7. Author(s)	8. Performing Organization Report No.
Harshvardhan and James A. Weinman	
9. Performing Organization Name and Address	10. Work Unit No.
National Aeronautics and Space Administration Goddard Space Flight Center, Greenbelt, MD 20771	11. Contract or Grant No. NAS5-26463
	13. Type of Report and Period Covered
12. Sponsoring Agency Name and Address	Technical Memorandum
	14. Sponsoring Agency Code

15. Supplementary Notes

16. Abstract

A study has been made of infrared radiative transfer through a regular array of cuboidal clouds considering the interaction of the sides of the clouds with each other and the ground. The theory is developed for black clouds and extended to scattering clouds using a variable azimuth two-stream (VATS) approximation. It is shown that geometrical considerations dominate over the microphysical aspects of radiative transfer through the clouds and simple analytical expressions are obtained to include finite cloud effects in flux and radiance computation.

17. Key Words (Selected by Author(s))	18. Distribution Statement
Infrared Emission Broken Cloud Array	

19. Security Classif. (of this report)	20. Security Classif. (of this page)	21. No. of Pages	22. Price*
Unclassified	Unclassified	14	

*For sale by the National Technical Information Service, Springfield, Virginia 22151.

GSFC 25-44 (10/77)